COMMISSIONING STATUS OF HIGH LUMINOSITY COLLIDER RINGS FOR SuperKEKB

H. Koiso, on behalf of the SuperKEKB Accelerator Team,
KEK, Tsukuba, Ibaraki, Japan

Abstract

The SuperKEKB project aims to obtain the world's highest luminosity of $8 \times 10^{35}\mathrm{cm}^{-2}\mathrm{s}^{-1}$, in order to discover new particle physics beyond the Standard Model. A key technologies is a low-emittance nano-beam scheme at the interaction point (IP) with high positron and electron stored currents, which requires significant upgrade of both the injector and the collider rings. This paper presents topical results from beam commissioning of the collider rings without final focus magnets and the Belle II detector (Phase 1), and construction status toward the first beam collisions (Phase 2).

INTRODUCTION

SuperKEKB [1] is an asymmetric-energy double-ring collider for 7 GeV electrons in the High Energy Ring (HER) and 4 GeV positrons in the Low Energy Ring (LER). It is a super B-factory upgraded from KEKB in order to quest for new physics beyond the Standard Model. The luminosity goal, 8×10^{35} $\mathrm{cm}^{-2}\mathrm{s}^{-1}$, is 40 times higher than the world's highest record at KEKB, and will be achieved by decreasing vertical beta functions at the IP, β_y^*s, to 1/20 of those at KEKB and by doubling the beam currents. Adopting the nano-beam scheme originally proposed by P. Raimondi [2], the longitudinal overlapping length of colliding bunches decreases to σ_x^*/θ_x (~250 μm). Thus β_y^*s can be squeezed to ~300 μm even with the bunch length of ~ 6 mm, avoiding the hourglass effect. To realize the nano-beam scheme, β_x^*s, emittances, and x-y emittance ratio also need to be significantly deceased from those at KEKB. The main machine parameters are summarized in Table 1.

Beam commissioning of the LER and HER is planned in three phases. In Phase 1, machine tuning and vacuum scrubbing are performed without the final focus superconducting magnet system (QCS) and the Belle II detector. In Phase 2, beam collision tuning starts with QCS and Belle II except the vertex detector. The target luminosity in Phase 2 is set to $\sim 1 \times 10^{34}\mathrm{cm}^{-2}\mathrm{s}^{-1}$. The full Belle II detector launches in Phase 3.

After 5.5 years of construction for the upgrade, the Phase 1 commissioning was carried out for 5 months from February to June in 2016. Among various results of Phase 1, this paper focuses on vacuum scrubbing, electron cloud issues, and the low emittance tuning. The construction status for Phase 2 will be also reported.

Table 1: Main Machine Parameters of SuperKEKB. The values in parentheses denote parameters without intra-beam scattering.

	LER (e+)	HER (e-)	units
Beam energy	4	7.007	GeV
Circumference	3016.315		m
Half crossing angle θ_x	41.5		mrad
Horizontal emittance	3.2 (1.9)	4.6 (4.4)	nm
Vertical emittance	8.60	11.5	pm
β_x^* / β_y^*	32 / 0.27	25 / 0.30	mm
σ_x^* / σ_y^*	10.1 / .048	10.7 / .062	μm
Energy spread	7.91	6.49	10^{-4}
Beam current	3.60	2.60	A
Number of bunches	2500		
Energy loss/turn	1.76	2.45	MeV
RF frequency	508.9		MHz
Bunch length	6.0	5.0	mm
Beam-beam param. (x)	0.0028	0.0012	
Beam-beam param. (y)	0.088	0.081	
Luminosity	8×10^{35}		$\mathrm{cm}^{-2}\mathrm{s}^{-1}$

PHASE-1 COMMISSIONING

Vacuum Scrubbing

The Phase 1 commissioning progressed smoothly as shown in Fig. 1 [3]. Hardware systems including newly introduced components basically worked as designed. With steady progress of the vacuum scrubbing, the beam currents reached 1.01 and 0.87 A, the average pressures ~ 1×10^{-6} and ~$2{\times}10^{-7}$ Pa, and the beam doses 780 and 660 Ah in the LER and HER, respectively [4]. The beam doses fully satisfied the requirements for installation of Belle II, which were to be greater than 360 Ah (0.5 A × one month) .

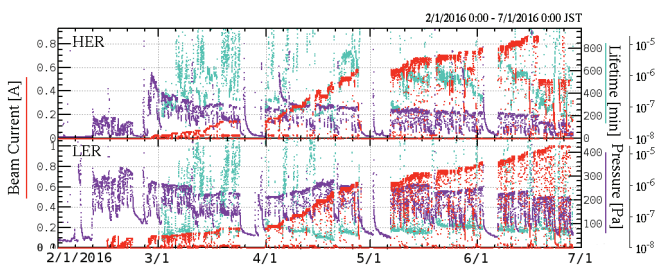

Figure 1: History of the Phase 1 commissioning of SuperKEKB. The red points denote the beam current, the purple the vacuum pressure, and the cyan the beam lifetime.

Copyright © 2017 CC-BY-3.0 and by the respective authors

ISBN 978-3-95450-182-3

Electron Cloud Effect

The single-bunch head-tail instability due to electron clouds in the LER was one of the most serious obstacles against achieving high luminosity at KEKB, and still is expected in SuperKEKB. As the countermeasures against the electron cloud effects and their results in Phase 1 have already been reported in detail in References [4–6], we outline the electron cloud issues according to these papers.

Various mitigations have been introduced for the beam pipes: the antechamber structure, TiN coating, grooved surfaces, clearing electrodes, and solenoid windings. Al-alloy beam pipes with the antechamber structure and with TiN coating on inner surface cover >90% of the LER in length. If all of these countermeasures are equipped, the average electron density all over the ring is expected to be $\sim 2\times10^{10}\mathrm{m}^{-3}$ at the design beam current of 3.6 A [5]. This value of the electron density is sufficiently low, compared with the threshold to excite the single-bunch instability, which is estimated to be $2\text{-}3\times10^{11}\mathrm{m}^{-3}$ [4,7,8]. However, the solenoid windings have not yet been installed in Phase 1. In the case without solenoids, the average electron density possibly increases to $\sim 6\times10^{11}\mathrm{m}^{-3}$, which is higher than the estimated threshold. Thus longitudinal magnetic fields by either solenoids or permanent magnets are indispensable to suppress the electron cloud effect.

The performance of the antechamber with TiN coating was demonstrated by measurements with electron current monitors which were placed in sections with and without TiN coating in a drift space. The Al-alloy antechamber with TiN coating successfully reduced the electron current as shown in Fig. 2 [4]. The electron current in the section with TiN coating was much lower than that without it when the beam current was high, which means that TiN coating effectively suppressed secondary electrons.

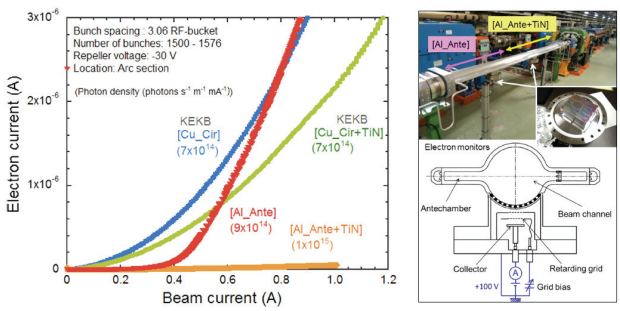

Figure 2: Electron current measurement [4].

In the early stage of Phase 1, the electron cloud effect was observed in the LER at a lower beam current than expected. When the beam current was ≥0.6 A, a nonlinear pressure rise and a blowup of the vertical beam size were observed. Actually there were Al-alloy bellows chambers without TiN coating were the main sources of the electron clouds, even though their total length was only ~5% of the entire ring (0.2 m × ~830). As a countermeasure, permanent magnets with longitudinal magnetic field of ~100 Gauss were attached to all of the Al-alloy bellows chambers. After installation of the permanent magnets, both the beam size blowup and the nonlinear pressure rise clearly slowed down as shown in Fig. 3 [4,6]. However, they were observed again at higher beam currents.

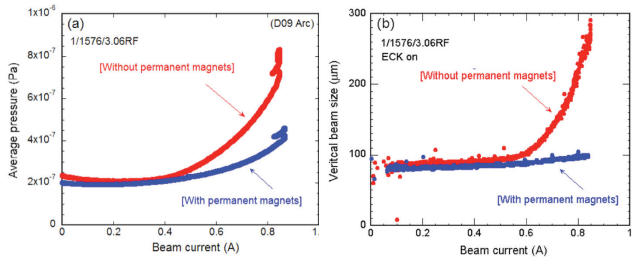

Figure 3: Nonlinear pressure rise (left) and vertical beam size blowup (right) due to the electron cloud effect [4].

The threshold beam current of the beam size blowup depends on a linear beam current density, which is defined as the bunch current divided by the bunch spacing in unit of the RF bucket (= 60 cm). In various bunch filling patterns, the beam size blowup occurred at almost same point in the linear current density as shown in Fig. 4 [6]. After having installed the permanent magnets, the threshold of the linear current density increased from 0.10-0.12 to 0.18-0.20 mA/bucket, while our goal is 0.72 mA/bucket (3600 mA/2500 bunches/2 buckets spacing).

The electron density in a drift space was estimated from the measurement with the electron current monitors mentioned above. The electron density in the region without coating was higher by one order of magnitude. Around the blowup threshold, the measured electron densities were not much different from simulation results [4, 6]. Further analysis will be reported elsewhere [9].

It was observed that the sideband spectrum of the vertical bunch oscillation changed from a "drift mode" to a "solenoid mode" before and after the installation of the permanent magnets. Even after the installation of the permanent magnets, however, the drift mode appeared again at higher beam current in the case of 2 bucket spacing [6]. Moreover the beam size blowup and the nonlinear pressure rise were also observed at higher beam current in the vacuum scrubbing with a usual filling pattern of 1/1576/3.06. These observations suggest that the electron clouds are still formed in drift spaces. It was confirmed that the pressure rise was relaxed locally in drift spaces where permanent magnets were attached for trial. Thus we will install permanent magnets in drift spaces all over the ring before Phase 2 [10]. Simulation studies to verify reduction of the electron density by permanent magnet installation are going on.

As for the maximum SEY, there is some discrepancy between simulations and measurements. Simulations suggest that the maximum SEY should be larger than ~1.3 averaged in the ring to excite the electron cloud effect in the LER with the present condition. On the other hand, measured values in the laboratory were 0.9-1.2 at the estimated electron dose

Copyright © 2017 CC-BY-3.0 and by the respective authors

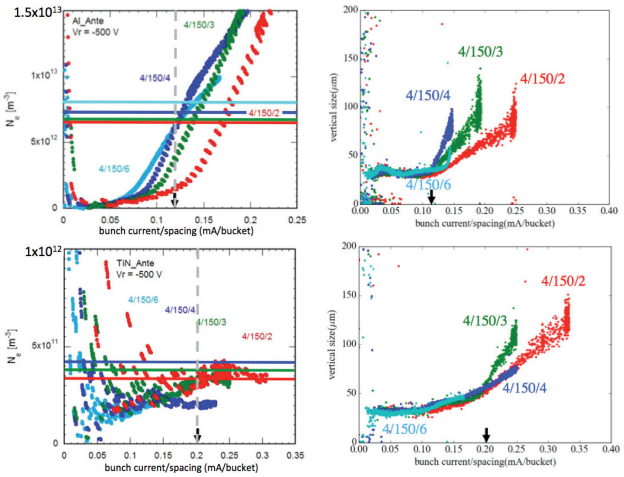

Figure 4: Dependence of the vertical beam size blowup (right) and the electron density estimated from the measurement with the electron current monitor (left) on the linear beam current density [6]. The lines in the left figures indicate simulation results at the blowup threshold. The filling pattern is expressed as, for example, 4/150/3 which means 4 trains, 150 bunches in a train, and 3 RF-bucket spacing.

of 5×10^{-4}C mm^{-2} [4, 6]. The reason for the discrepancy has not yet been understood. Some possibilities are pointed out: more dose of electrons with sufficient energies or lower pressure in the beam pipes may be necessary, or there still remain places where the electron density is locally high. Further investigation will be conducted in Phase 2.

Low Emittance Tuning

Optics corrections in Phase 1 have been worked successfully in both rings [11]. Skew quadrupole-like corrector windings on sextupole magnets (Fig. 5) are newly introduced at SuperKEKB for optics correction. The sextupoles are placed as noninterleaved pseudo $-I$ pairs all over the ring. So the skew quadrupole-like correctors on a sextupole pair are also connected by the pseudo $-I$ transformation. Then x-y couplings and vertical dispersion can be corrected almost independently by using symmetric and asymmetric excitation of the skew quadrupole corrector in a pair. For x-y coupling correction, the vertical orbits excited by horizontal steering magnets were corrected as shown in Fig. 5. Results of the optics correction were: $(\Delta y)_{\rm rms}/(\Delta x)_{\rm rms}$ = 0.9 and 0.6 %, $(\Delta\eta_x)_{\rm rms}$ = 8 and 11 mm, in the LER and HER, respectively, $(\Delta\eta_y)_{\rm rms}$ = 2 mm, $(\Delta\beta_x/\beta_x)_{\rm rms}$ = 3 %, $(\Delta\beta_y/\beta_y)_{\rm rms}$ = 3 % in both rings, which are sufficiently small to start optics tuning with QCS.

A tentative goal of the vertical emittance ε_y has been achieved in the LER as shown in Fig. 6. The vertical emittances were estimated from the beam sizes measured by X-ray monitors (XRMs), which were newly introduced for SuperKEKB to measure smaller beam sizes than by visible SR monitors. In the HER, measurements with the XRM brought about larger ε_y than that expected from the optics

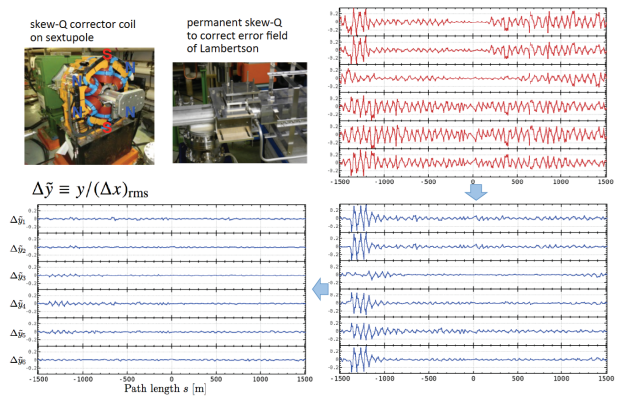

Figure 5: Example of the x-y coupling correction in the LER [11]. In addition to usual correctors, a localized coupling source was corrected by additional permanent skew quadrupole magnets.

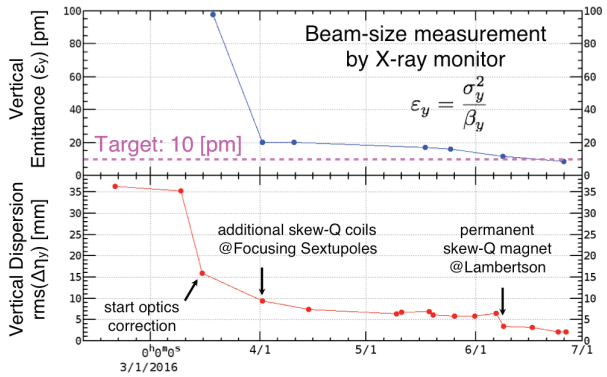

Figure 6: Progress of the optics correction in the LER during Phase 1 commissioning [11].

correction. More calibration of the XRM and enlarging β_y at the XRM will be done in Phase 2.

CONSTRUCTION STATUS FOR PHASE 2 COMMISSIONING

QCS

In order to achieve the extremely small β_y^*, a very precise and complicated final-focus magnet system has been constructed. Based on the requirements from beam optics design [12], QCS has been built as a complex consisting of a number of superconducting magnets: main quadrupole magnets, various kinds of corrector magnets, and compensation solenoids as shown in Figs.7, 8 and 9 [13].

All of the quadrupole magnets have multi-layer corrector magnets. The corrector magnets were constructed by BNL under the research collaboration. With BNL's special technique, direct winding method, the superconducting coils were wound directly on the helium inner vessel [14]. The following types of corrector magnets are equipped: normal and skew dipoles (b1 and a1) to correct horizontal and vertical displacements of the quadrupole, skew quadrupole (a2) to correct rotation error of the quadrupole, normal and skew

Copyright © 2017 CC-BY-3.0 and by the respective authors

ISBN 978-3-95450-182-3

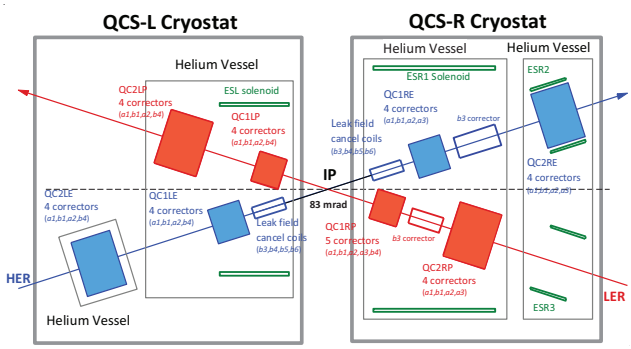

Figure 7: Conceptual design of QCS [13]. Fifty-five superconducting magnets (8 main quadrupole magnets, 43 corrector magnets, and 4 compensation solenoids) are assembled in the two cryostats, QCSL and QCSR.

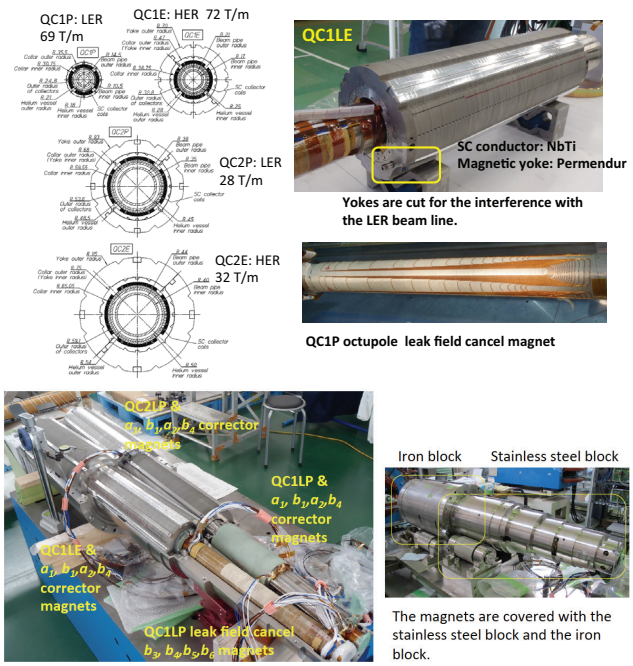

Figure 8: Cross sections of the main quadrupole magnets (upper left) [13] and the construction of QCS (I). QC1E, QC2P, and QC2E have Permendur yokes.

sextupoles (b3 and a3) to cancel the sextupole fields induced by the assembly errors of the quadrupoles, normal octupole (b4) to optimize the dynamic apertures. The leak field cancel magnets (sextupole, octupole, decapole, dodecapole) cancel nonlinear components of the leak field from QC1P to the HER beam line because QC1Ps have no magnetic yokes. The linear components of the leak field are taken into account for optics design.

The compensation solenoids cancel the Belle II solenoid field so that the integrated solenoid field should be zero on each side of the IP as shown in Fig. 9. The field profile of the solenoids is so optimized as to minimize the vertical emittance and is realized by combining small segments of

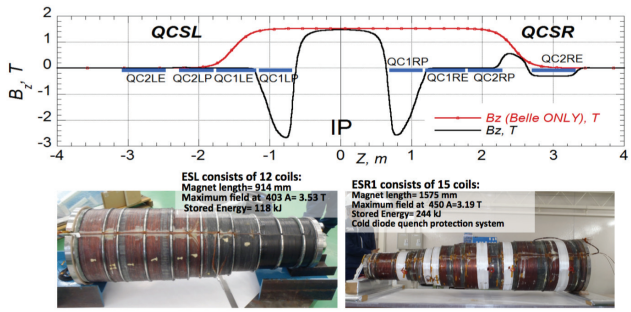

Figure 9: The compensation solenoids.

solenoid coils. Tungsten-alloy radiation shields surrounds the compensation solenoids as shown in Fig. 10.

Figure 10: The construction of QCS (II).

The construction of the QCS cryostats was completed, and the two cryostats and the cryogenic systems were integrated on the both sides of the interaction region (IR) in March 2017 (Fig. 11). Then the Belle II detector was rolled in on April 11. The commissioning and field measurements of the QCS-L and QCS-R systems with the Belle solenoid field are scheduled from May to August 2017.

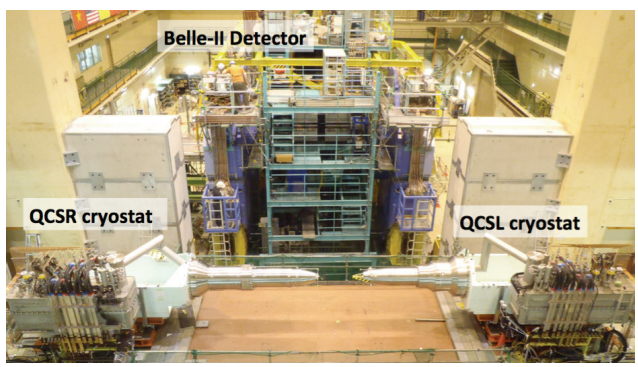

Figure 11: The status of the IR before roll in of the Belle II detector.

Positron Damping Ring

In order to produce a low-emittance positron beam for good injection to the LER, a positron damping ring is being newly constructed as shown in Fig. 12 [15, 16]. A novel "reverse-bend FODO" cell has been developed to achieve

Copyright © 2017 CC-BY-3.0 and by the respective authors

sufficiently short damping time [17]. Magnets, their power supplies, beam pipes, RF cavities, etc. have already been installed. Installation of ECS, BCS, kickers, and septums, fine alignment of magnets, high power conditioning of RF cavities, adjustments of magnet power supplies etc. will be performed from now on.

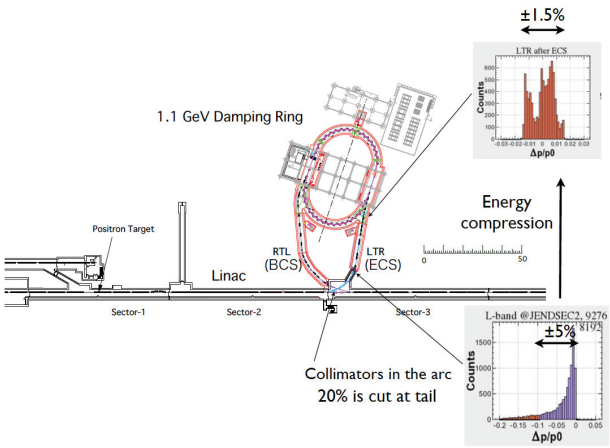

Figure 12: System layout of the positron damping ring [16].

Table 2: Parameters of the Positron Damping QRing [16]

Beam energy	1.1	GeV
Circumference	135.498295	m
Horizontal damping time	11.57	ms
Injected-beam emittance	1400	nm
Equilibrium emittance (h/v)	41.5 / 2.08	nm
Emittance at extraction (h/v)	42.9 / 3.61	nm
Energy spread	5.5×10^{-4}	

Overall schedule of SuperKEKB is shown in Fig. 13. The commissioning of the damping ring will start earlier than that of the collider rings so as that high-quality positron beams from the injector can be ready for first beam commissioning of QCS and Belle II.

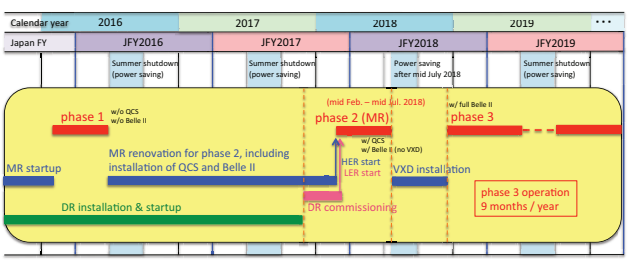

Figure 13: Overall schedule of SuperKEKB

SUMMARY

The Phase 1 commissioning of SuperKEKB collider rings was performed successfully. Beam doses sufficient for Belle II roll-in were achieved.

Electron cloud effects are not so different from expectation. The new beam pipes with antechamber structure and TiN coating worked well. A reduction of secondary electrons by TiN coating was clearly observed. Without longitudinal magnetic fields, electron clouds were still formed in drift spaces with antechambers and TiN coating. Then permanent magnets will be attached to drift spaces all over the ring before the Phase 2 commissioning. More simulations on the effect of the permanent magnets are going on. Further studies on SEY will be performed in Phase 2.

Construction for Phase 2 are steadily in progress. QCS and Belle II has been installed in the IR. The Phase 2 commissioning will start soon: the positron damping ring will start in late 2017, and the collider rings with QCS and Belle II in mid February in 2018.

ACKNOWLEDGMENT

The author would like to thank the colleagues of SuperKEKB Accelerator Team for their intensive discussions and helping with this report.

REFERENCES

[1] Preliminary version of Technical Design Report of SuperKEKB, https://kds.kek.jp/indico/event/15914/

[2] P. Raimondi, 2nd SuperB Meeting, Frascati (2006).

[3] Y. Funakoshi, "Commissioning of SuperKEKB", presented at eeFACT2016, Daresbury, UK, October 2016, paper MOOTH2.

[4] Y. Suetsugu *et al.*, *J. Vac. Sci. Technol.* A 35, 03E103 (2017).

[5] Y. Suetsugu *et al.*, *J. Vac. Sci. Technol.* A 34, 021605 (2016).

[6] H. Fukuma *et al.*, "Electron cloud at SuperKEKB", presented at eeFACT2016, Daresbury, UK, October 2016, paper TUT3AH6.

[7] Y. Susaki and K. Ohmi, "Electron cloud instability in SuperKEKB low energy ring", in *Proceedings of the IPAC'10*, Kyoto, Japan, pp. 1545-1547.

[8] K. Ohmi and D. Zhou, "Study of electron cloud effects in SuperKEKB", in *Proceedings of the IPAC'14*, Dresden, Germany, pp. 1597-1599.

[9] K. Ohmi *et al.*, presented at IPAC2017, Copenhagen, Denmark, paper WEPIK075, this conference.

[10] Y. Suetsugu *et al.*, presented at IPAC2017, Copenhagen, Denmark, paper WEPIK008, this conference.

[11] Y. Ohnishi *et al.*, "Optics correction and low emittance tuning at the phase 1 commissioning of SuperKEKB", presented at eeFACT2016, Daresbury, UK, October 2016, paper TUT3BH2.

[12] H. Sugimoto, "Design study of the SuperKEKB interaction region optics", in *Proceedings of the IPAC'14*, Dresden, Germany, pp. 950-952.

[13] N. Ohuchi *et al.*, "Design of the superconducting magnet system for the SuperKEKB interaction region", in *Proceedings of the NA-PAC'13*, Pasadena, CA USA, pp. 759-761.

Copyright © 2017 CC-BY-3.0 and by the respective authors

ISBN 978-3-95450-182-3

[14] B. Parker, "Direct wind superconducting corrector magnets for the SuperKEKB IR", in *Proceedings of the IPAC'12*, New Orleans, Louisiana, USA, pp. 2191-2193.

[15] M. Kikuchi *et al.*, "Design of positron damping ring for SuperKEKB", in *Proceedings of the IPAC'10*, Kyoto, Japan, pp. 1641-1643.

[16] M. Kikuchi, a talk given at the *21st KEKB Accelerator Review Committee Meeting* (2016).

[17] M. Kikuchi, "Reverse-bend FODO lattice applied to damping ring for SuperKEKB", *Nucl. Instr. Meth.* A 556, pp.13-19 (2006).

Copyright © 2017 CC-BY-3.0 and by the respective authors

ISBN 978-3-95450-182-3